Chinese Chemical Letters 36 (2025) 110438

Contents lists available at ScienceDirect

Chinese Chemical Letters

journal homepage: www.elsevier.com/locate/cclet

Application of titanium-based advanced oxidation processes in pesticide-contaminated water purification: Emerging opportunities and challenges

Chu Wu[a,1], Zhichao Dong[b,c,1], Jinfang Hou[b,c], Jian Peng[d,e], Shuangyu Wu[d,e], Xiaofang Wang[a], Xiangwei Kong[a], Yue Jiang[d,e,*]

[a] Wenzhou Key Laboratory of Soil Pollution Prevention and Control, Zhejiang Industry & Trade Vocational College, Wenzhou 325003, China
[b] Tianjin Port Engineering Institute Co., Ltd. of CCCC First Harbor Engineering Co., Ltd, Tianjin 300222, China
[c] CCCC First Harbor Engineering Company Ltd., Tianjin 300461, China
[d] College of Environmental Science and Engineering, Biomedical Multidisciplinary Innovation Research Institute, Shanghai East Hospital, Tongji University, Shanghai 200092, China
[e] Key Laboratory of Yangtze River Water Environment, Shanghai Institute of Pollution Control and Ecological Security, Tongji University, Shanghai 200092, China

ARTICLE INFO

Article history:
Received 3 June 2024
Revised 5 September 2024
Accepted 9 September 2024
Available online 10 September 2024

Keywords:
Emerging contaminants
Atrazine
Titanium-based nanomaterial
Advanced oxidation processes
Sustainable-by-design

ABSTRACT

Efficient and innovative nano-catalytic oxidation technologies offer a breakthrough in removing emerging contaminants (ECs) from water, surpassing the limitations of traditional methods. Environmental functional materials (EFMs), particularly high-end oxidation systems using eco-friendly nanomaterials, show promise for absorbing and degrading ECs. This literature review presents a comprehensive analysis of diverse traditional restoration techniques-biological, physical, and chemical-assessing their respective applications and limitations in pesticide-contaminated water purification. Through meticulous comparison, we unequivocally advocate for the imperative integration of environmentally benign nanomaterials, notably titanium-based variants, in forthcoming methodologies. Our in-depth exploration scrutinizes the catalytic efficacy, underlying mechanisms, and adaptability of pioneering titanium-based nanomaterials across a spectrum of environmental contexts. Additionally, strategic recommendations are furnished to surmount challenges and propel the frontiers of implementing eco-friendly nanomaterials in practical water treatment scenarios.

1. Introduction

The distinguishing aspect of "emerging" in emerging contaminants (ECs) lies not merely in their novelty of synthesis but rather in their recent discovery or heightened recognition due to their potential ecological and human health threats. Regrettably, prevailing pollution treatment and environmental management paradigms frequently disregard ECs, resulting in a failure to mitigate associated environmental hazards [1,2]. The ECs commanding global attention primarily encompass endocrine disrupting chemicals (EDCs), persistent organic pollutants (POPs), antibiotics, and microplastics. In contrast to conventional pollutants, ECs exhibit a spectrum of characteristics-diverse in type, pervasive in origin, resistant to degradation, prone to ecosystem accumulation, and marked by enduring persistence in the environment and organisms. These inherent traits underscore the potential ecological health risks they pose [3-5].

EDCs, exemplifying emerging contaminants, pervade multiple spheres of human activity and production [6]. China, a key grain producer, has historically employed common EDCs such as atrazine (ATZ) as pesticides to manage herbaceous weeds in staple crops like cotton, corn, soybean, rice, and wheat. Analysis conducted across 28 sites within the Yangtze River Delta unveiled ATZ concentrations surpassing average European annual levels, with a maximum concentration of 1726 ng/L, marking a 9.4-fold increase from surface water detections [7,8]. Prolonged exposure to these EDCs heightens the risk of reproductive disorders [9,10], cognitive impairments [11], metabolic dysfunctions [12] and diverse cancers [13]. Recent reports advocate a comprehensive health risk assessment framework for EDCs, anchored in previously identified car-

* Corresponding author.
E-mail address: jiangyue81@tongji.edu.cn (Y. Jiang).
[1] These authors contributed equally to this work.

https://doi.org/10.1016/j.cclet.2024.110438
1001-8417/

cinogenic attributes [14]. This framework hinges on the physical and chemical properties of EDCs, integrating designated traditional methods tailored to each property. These methods are broadly categorized into biological, physical, and chemical treatments. Simultaneously, ongoing advancements aim to optimize these treatment techniques [15]. Concomitantly, the evolution of nanotechnology has underscored the potential of environmental nano-catalytic oxidation technologies in effectively mitigating EDCs, representing a significant departure from conventional methodologies [16].

This literature review meticulously delineates the mechanisms, exemplars, and existing limitations of conventional treatment methodologies using ATZ as a typical emerging contaminant. We provide a concise summary of their contexts and delve deeply into investigating whether the innovative nano-catalytic oxidation technology, integrating EFMs can transcend the confines of these established approaches. With a specific focus on titanium-based nanomaterials, we scrutinize their environmental efficacy, catalytic mechanisms, and scope for application. The core objective of this article is aim to develop a more comprehensive strategy for green, safe restoration techniques as well as actual engineering practice inspired by the concept of "Sustainable-by-design" [17,18].

2. Traditional water treatment and restoration technology

2.1. Biological technique

The application of biological techniques, employing microorganisms as the principal agents, is widespread in addressing environmental organic pollutants. Global researchers have cataloged a spectrum of microorganisms proficient in degrading ATZ pesticides, with their specific degradation performances detailed in Table S1 (Supporting information) [19-26].

Microbial restoration techniques stand out for their versatility, ease of operation, cost-efficiency, and minimal secondary environmental impact. However, their effectiveness is hampered by the susceptibility of microorganism growth to environmental variables like temperature, salinity, and pH. Hence, the ongoing imperative lies in identifying microorganisms demonstrating superior performance and heightened environmental resilience.

2.2. Physical technique

2.2.1. Adsorption

Adsorption remains the predominant physical technique employed in wastewater treatment [27,28]. Utilized adsorbents typically exhibit a high specific surface area, facilitating the swift adsorption of ECs from wastewater. Presently, adsorbents comprise various materials including activated carbon, bio-carbon, agricultural solid waste, industrial by-products, natural clay minerals, and biological adsorbents. These adsorbents have showcased notable effectiveness in the efficient removal of pesticide residues from water [29,30].

Studies have demonstrated the effectiveness of polyaniline-derived carbon (PDC) in adsorbing ATZ [31]. Scientific findings indicate that PDC, produced *via* pyrolysis at 800 °C, exhibits a maximum ATZ adsorption capacity of 943 mg/g, surpassing active carbon (AC) by 7.7 times under similar conditions. Phosphorus-doped biochar, derived from single-step pyrolysis of corn straw, demonstrates a maximum ATZ adsorption capacity of 79.6 mg/g and remains usable for up to 5 cycles [32]. Additionally, biochar with smaller particle sizes significantly accelerates the attainment of adsorption equilibrium, while lower pH levels exert a pronounced influence. These observed trends align consistently with the Freundlich model (Fig. S1 in Supporting information) [33].

2.2.2. Membrane filtration

Membrane filtration relies on membranes with diverse aperture sizes to effectively filter and segregate substances based on their size and thrust, a method extensively utilized in EDC removal. Using polyamide micro/nano membranes for ATZ retention, standalone membranes exhibit a mere 17% removal efficiency, which significantly escalates to 92.23% with the incorporation of functional layers crafted from chitosan/polystyrene sulfonate, particularly reaching this efficacy with 9 layers. Notably, the introduction of humus displays minimal impact on membrane properties, whereas the presence of Ca^{2+} substantially hampers membrane performance [34]. Investigations employing commercialized nano-filtration membranes for ATZ retention reveal nanofiltration membrane 90 (NF90) as the most effective, achieving a removal efficiency of 95%, followed by nanofiltration membrane 200 (NF200) and DK at 75%, while nanofiltration membrane 270 (NF270) maintains an approximately 60% removal efficiency. Furthermore, heightened pressure significantly enhances the performance of nano-filtration membranes (Fig. S2 in Supporting information) [35].

2.2.3. Coagulation/flocculation/precipitation

Coagulation, flocculation, and precipitation methods typically isolate pollutants in sediment form by employing lime, alum, iron salts, and polymers. Nonetheless, these substances incur relatively high costs with a comparatively modest pollutant removal rate. Moreover, the sediments generated through coagulation, flocculation, and precipitation necessitate subsequent secondary treatment [36,37].

2.3. Chemical technique

2.3.1. Chlorination

The components involved in chlorination typically encompass cost-effective chlorine and hypochlorite. Among these constituents, hypochlorite boasts the highest standard oxidation potential, reaching 1.48 V, followed by chlorine gas and chlorine dioxide at 1.36 V and 0.95 V, respectively [38]. The hydrolysis of chlorine in water, as represented by reaction Eq. 1, delineates the generation of hypochlorous acid (HOCl) upon dissolution in water. Subsequently, HOCl engages with organic compounds through mechanisms including unsaturated bond addition, electrophilic substitution, and oxidation reactions [39]. However, this reaction pathway often results in the formation of by-products with carcinogenic potential, notably haloacetic acid and trihalomethane [40]. Furthermore, there is a potential risk associated with the incomplete elimination of residual ECs in water.

$$Cl_2 + H_2O \rightarrow HOCl + Cl^- + H^+ \quad (1)$$

Current literature is scarce concerning the use of this technique for pesticide pollutant treatment. Chlorination, often combined with other methods due to its limited efficacy when employed in isolation, has shown a compelling synergistic effect when paired with ammonification, achieving a 50.2% degradation of ATZ within 10 min. The identified intermediates suggest that ATZ degradation involves dealkylation and dechlorine-hydroxylation processes. Comparatively, the combined ammonification and chlorination process yields lower oxidative by-products than chlorination alone [41]. Moreover, the amalgamation of illumination and chlorination demonstrates effectiveness in treatment. While individual applications of illumination or chlorination struggle to sufficiently degrade ATZ, their combined utilization achieves a 65% degradation efficiency. Remarkably, this amalgamated approach circumvents inhibition by natural organisms and can even benefit from compounds

such as bromides which can be used as raw materials or intermediates in the preparation of certain drugs (Fig. S3 in Supporting information) [42].

2.3.2. Ozonation

Ozone, recognized as a potent oxidizer ($E_0 = 2.07$ V), surpasses chlorine in its oxidation potential. This makes it highly effective for purifying mobile and fluid water [43]. Upon dissolving in water, ozone undergoes decomposition, yielding hydroxyl radicals ($^{\bullet}OH$), pivotal for mineralizing pollutants [44]. The reaction formulas corresponding to this process are delineated in reaction Eqs. 2–7.

$$O_3 + OH^- \rightarrow O_2 + HO_2^- \quad (2)$$

$$O_3 + HO_2^- \rightarrow HO_2^{\bullet} + O_3^{\bullet -} \quad (3)$$

$$HO_2^{\bullet} \rightarrow H + O_2^{\bullet -} \quad (4)$$

$$O_2^{\bullet -} + O_3 \rightarrow O_2 + O_3^{\bullet -} \quad (5)$$

$$O_3^{\bullet -} + H \rightarrow HO_3^{\bullet} \quad (6)$$

$$HO_3^{\bullet} \rightarrow {}^{\bullet}OH + O_2 \quad (7)$$

Presently, ozone has been employed for the oxidation and mitigation of pesticide-related compounds to some extent. Nonetheless, studies highlight the insufficiency of ozone's oxidative activity when used in isolation. Fortunately, the incorporation of catalysts has proven effective in augmenting oxidation. For instance, the integration of a finely compounded catalyst featuring graphitic carbon and nitride into the oxidation system significantly enhances the ATZ degradation efficiency by 29.76% compared to ozone oxidation alone [45]. Similarly, investigations reveal that while the ATZ removal rate remains at 27% during ozone oxidation in isolation, it escalates to 98% within a tourmaline ozonation system after a 10 min reaction period (Fig. S4 in Supporting information) [46].

2.3.3. Photolysis

Photolysis, leveraging both natural and artificial light sources, facilitates the decomposition or dissociation of compounds through direct or indirect pathways [47]. Direct photolysis entails the reaction of pollutants with water-based groups or their spontaneous decomposition under ultraviolet radiation. Conversely, indirect photolysis harnesses the oxidation of photosensitizers (such as oxyradicals, hydroxyl radicals, and peroxy radicals), with the entire process markedly influenced by the half-life of free radicals [48,49]. Generally, both direct and indirect photolysis mechanisms can concurrently take place.

Empirical evidence underscores the impact of chemical structure on the photolytic process, revealing the relatively facile degradation of common photosensitive compounds [50,51]. Nonetheless, the standalone efficacy of photolysis in degradation remains relatively limited. Consequently, it is frequently complemented by techniques involving hydrogen peroxide (H_2O_2) and ozone (O_3). Studies indicate that ATZ degradation efficiency reaches only 40% in pure UV photolysis, but increases to 70% in UV/Cl_2 photolysis [52].

The aforementioned review highlights the limited efficacy of pure photolysis in degrading pesticides' pollutants. Consequently, this technique finds optimal application in treating wastewater containing photosensitive substances or characterized by low COD concentrations, including scenarios like river water, drinking water, and analogous contexts.

2.3.4. Electrochemical oxidation

Electrochemical treatment is essentially a conversion from electrical energy into chemical energy. It is also currently used in EC treatment [53]. In the electrochemical degradation of ATZ, utilizing boron-doped diamond as the anode (compared to a Pt electrode) results in an 82% degradation efficiency after 10 h of reaction [54]. When employing multi-walled carbon nanotubes coated with binuclear iron phthalocyanine as a non-inert catalyst at the anode, effective dechlorination of ATZ is achieved. Additionally, ATZ degradation is markedly pH-dependent. Initially, the degradation efficiency rises with decreasing pH values, but it begins to decline after the pH 1.5 (Fig. S5 in Supporting information) [55].

2.3.5. Sulfate radical oxidation

Sulfate radical ($SO_4^{\bullet -}$) oxidation stands as a recently developed, advanced oxidation technique. Its mechanism involves the activation of persulfate (PS) or peroxonosulfate (PMS) through light, heat, or metal ions, culminating in the production of $SO_4^{\bullet -}$. This radical subsequently effectively mineralizes pollutants. Comparatively, the oxidation process facilitated by $SO_4^{\bullet -}$ is less influenced by pH value, touting a higher redox potential ($E_0(SO_4^{\bullet -}/SO_4^{2-}) = 2.44$ V) and displaying greater selectivity towards pollutants. Consequently, the degradation process remains minimally disrupted by impurities dissolved in water, such as organisms. Moreover, $SO_4^{\bullet -}$ boasts a longer half-life in pure water than $^{\bullet}OH$ (with a half-life of 40 μs for $SO_4^{\bullet -}$ *versus* 20 ns for $^{\bullet}OH$), affording extended reaction time with the target pollutant [56].

In the degradation process of ATZ, the activation of PS by Fe^{2+} has demonstrated effectiveness in enhancing ATZ degradation efficiency [57]. Studies have investigated various conditions to discern the patterns and mechanisms involved in ATZ degradation. Particularly, experiments were conducted using a self-developed composite material comprising graphene and nano-scale zero-valent iron (nZVI/GR) to activate PS. The findings reveal that the 92.1% ATZ removal is achieved at a mass ratio of 5:1 for nZVI/GR in 21 min (Fig. S6 in Supporting information) [58].

Activation of PS through diverse methods yields varying activation efficiencies. Excessive PS usage introduces sulfate radicals into the system, triggering acidification and secondary pollution.

2.3.6. Photocatalysis

Photocatalysis is a process of converting solar energy into chemical energy [59]. Its mechanism can be described by three steps (Fig. S7 in Supporting information):

Based on the outlined mechanism, W-TiO_2/clay photocatalyst was successfully synthesized using a straightforward sol–gel method. This composite demonstrates efficient ATZ removal under sunlight exposure, achieving a remarkable 90% degradation efficiency within 4 h of reaction [60]. Similarly, under UV irradiation, Bi_2O_3 exhibits an impressive ATZ removal efficiency of 92.1% within 60 min [61].

The extensive discourse on photocatalytic oxidation and its industrial viability stems from its utilization of an inexhaustible clean energy source, *i.e.*, solar energy, to generate highly oxidizing free radicals [62]. This process exhibits promising potential for efficiently eliminating organic pollutants from rivers, groundwater, and drinking water. Moving forward, emphasis should be placed on enhancing light accessibility, augmenting the oxidizing impact, ensuring safety, and establishing efficient recycling methods for the widely employed commercial photocatalyst (P25).

2.3.7. Homogeneous Fenton oxidation

In the late 19th century, chemist Fenton made a pivotal discovery, observing the potent oxidizing ability of the combination of H_2O_2 and iron against organisms. This discovery led to the term "Fenton system" for this process [63]. Subsequent advancements

were made by Barb *et al.*, refining its reaction mechanism [64]. Building on this foundation, subsequent researchers conducted extensive studies, culminating in the establishment of the chain Fenton reaction mechanism for the degradation of organic pollutants, a widely accepted model within the scholarly community [44]. The chain reaction equations are detailed as follows (Eqs. 8–13):

$$Fe^{2+} + H_2O_2 \rightarrow Fe^{3+} + OH^- + {}^{\bullet}OH \quad (8)$$

$$Fe^{3+} + H_2O_2 \rightarrow Fe^{2+} + H^+ + HOO^{\bullet} \quad (9)$$

$$Fe^{3+} + HOO^{\bullet} \rightarrow Fe^{2+} + H^+ + O_2 \quad (10)$$

$$Fe^{2+} + {}^{\bullet}OH \rightarrow Fe^{3+} + OH^- \quad (11)$$

$$H_2O_2 + {}^{\bullet}OH \rightarrow H_2O + HOO^{\bullet} \quad (12)$$

$${}^{\bullet}OH + \text{organic pollutant} \rightarrow CO_2 + H_2O \quad (13)$$

As a consequence, traditional homogeneous reactions have not gained widespread use. Ongoing studies explore modifications, such as incorporating photolysis into the system, resulting in a modified photo-Fenton system that moderately enhances degradation efficiency [65]. Nonetheless, the photo-Fenton system is generally unsuitable for treating sewage with high organic content due to turbidity, which obstructs UV penetration and radiation.

2.3.8. Heterogeneous Fenton-like oxidation

To surmount the constraints posed by traditional homogeneous Fenton oxidation-excessive formation of iron sludge, constrained H_2O_2 utilization, a limited effective pH range, and intricate catalyst recycling-heterogeneous Fenton-like oxidation has emerged [66]. This method stands out due to its capability to immobilize metal ions with varying valence, yielding metal oxides, metals, and solid catalysts supported or doped with metals. Developed on the premise of solid-phase catalysts efficiently decomposing H_2O_2 to oxidize substances and subsequently mineralize organic compounds, this technique operates based on the following chain reaction equations (Eqs. 14–16):

$$\equiv M^{n+} + H_2O_2 \rightarrow \equiv M^{(n+1)+} + OH^- + {}^{\bullet}OH \quad (14)$$

$$\equiv M^{(n+1)+} + H_2O_2 \rightarrow \equiv M^{n+} + H^+ + HOO^{\bullet} \quad (15)$$

$$HOO^{\bullet} + M^{(n+1)+} \rightarrow \equiv M^{n+} + H^+ + O_2 \quad (16)$$

Building on previous homogeneous Fenton oxidation reactions, Fe-based catalysts were initially explored. A composite system of Fe(III)-ATTP-PANI was created through vapor deposition. Under a constant pH 3, 10.0 μmol/L of ATZ could be completely degraded within 40 min, maintaining a removal efficiency of over 90% even after 6 rounds of recycling [67]. Additionally, employing Fe-supported carbon-based catalysts derived from microplastics as raw material achieved a degradation rate of 83% for tetracycline (40 mg/L) within 10 min at a pH 4.3 [68].

While recent heterogeneous catalysts have made strides in mitigating issues such as heightened H_2O_2 consumption and challenging catalyst recycling, the present system's efficacy remains confined to an acidic environment. Concurrently, the seepage of Fe(III) into the solution and its adhesion to the Fe base lead to reactions with OH^-, resulting in substantial iron sludge formation, indicating that stability concerns within the reaction persist. Seeking further advancement beyond Fe-based Fenton catalysts, researchers have progressively explored diverse transition metal elements with varying valence (*e.g.*, Cu and Ni) to supplant Fe^{2+} and accelerate H_2O_2 decomposition. Notably, specific studies have detailed the synthesis of a Ni-doped composite material, FeO_x (Ni@FeO_x), employing a hydrothermal approach, showcasing its prowess in catalyzing H_2O_2 decomposition. Remarkably, this catalyst achieved a 90% removal of DDT pesticide within an 8-h duration. The principal mechanism involves the collaborative role of Ni^{2+}/Ni^0 and Fe^{3+}/Fe^{2+} in bimetallic catalysis, markedly amplifying H_2O_2 decomposition and bolstering the generation of oxidizing free radicals [69].

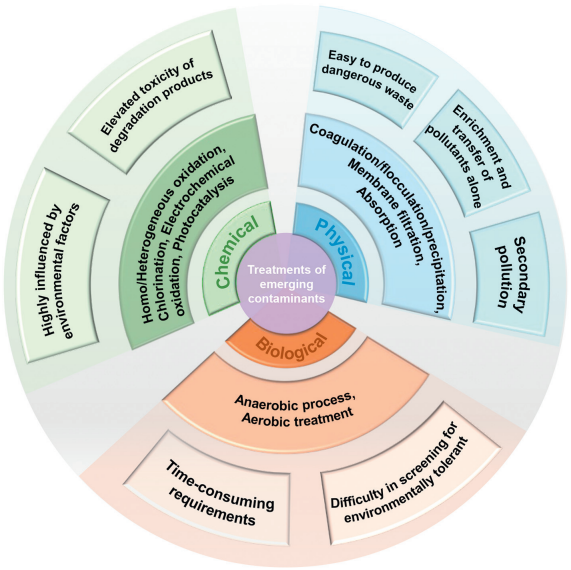

Fig. 1. Traditional water treatment technologies and their existing defects.

While harnessing the potential of effective environmental functional materials, steadfast adherence to the "Safer-by-design" principle remains paramount. Consequently, the future strides in Fenton-like catalysis pivot on the quest for safer Fenton-like oxidation systems, bolstering material stability, refining catalytic performance, and ensuring adaptability across a wide pH spectrum [70].

3. A comparison between the techniques

Through the aforementioned discussion, it becomes apparent that present biological techniques heavily hinge on microorganisms rendering them highly vulnerable to environmental constraints. Thus far, the identification of microorganisms exhibiting broad environmental resilience applicable across diverse practical settings remain elusive. Furthermore, the extended timeframes required for biological degradation render these methods impractical for emergency treatments. Conversely, physical techniques facilitate the enrichment and transfer of pollutants without achieving comprehensive elimination. Consequently, the transformation of employed functional materials into hazardous waste compounds amplifies environmental risks and incurs elevated disposal costs (Fig. 1).

Taking into account parameters like oxidation efficiency, the extent of pollutant mineralization, and versatility, chemical techniques emerge as more suitable and competitive for water treatment. In consonance with the tenets of green restoration and "Safer-by-design", we endorse the prioritization of photocatalytic oxidation utilizing renewable energy sources such as solar energy,

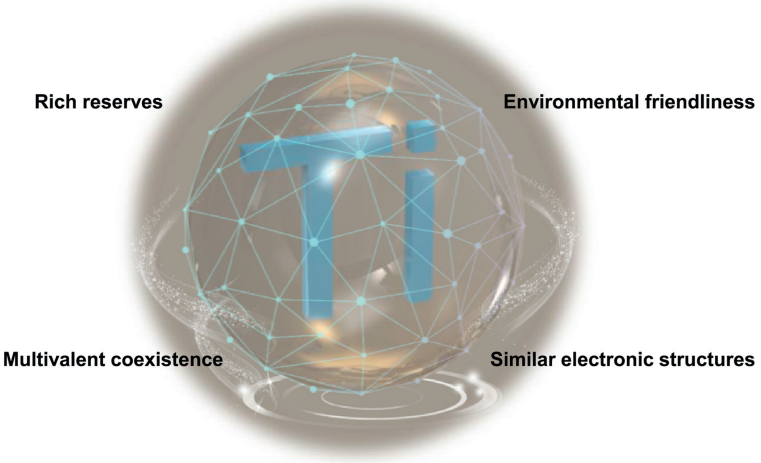

Fig. 2. Advantages of titanium-based nanomaterials: (1) Rich reserves. (2) Environmental friendliness. (3) Similar electronic structures to Fe element. (4) The potential of Fenton-like catalysis due to the multivalent coexistence.

as well as Fenton-like catalytic systems relying on H_2O_2 oxidation. Our advocacy is grounded in the following rationale:

(1) Photocatalysis can stimulate the production of oxidizing substances purely by light, which is a type of green energy; compared with $SO_4^{\bullet-}$, the final products of $^{\bullet}OH$ only include H_2O and CO_2, which do not cause acidification and are thus green;
(2) Both methods produce free radicals with strong oxidation capacity (such as $^{\bullet}OH$, $O_2^{\bullet-}$, $^1O_2$), which can effectively mineralize pollutants and reduce intermediates coupled with potential safety problems if treated incompletely;
(3) Current photocatalytic materials have been successfully commercialized and marketed, and Fenton oxidation based on $^{\bullet}OH$ has already been applied in sewage treatment plants. The practical experience so far and advantages contribute to a huge application potential;
(4) The shared core of both techniques is multi-functional nanomaterials. And the design, manufacturing, and application promotion of nanomaterials are highly expected. Admittedly, the introduction of any new system will inevitably bring more challenges. In the follow-up studies, it is suggested to focus on the simplification of material preparation, the optimization of the efficiency, stability, and safety of the materials, and further exploration of reaction mechanism and application potential in the environment;
(5) Advanced oxidation can also be effectively combined with biological techniques as pretreatment. By advanced oxidation, pollutants are first turned into intermediates that are easy to biodegrade and less toxic, and then further treated by biological techniques. Another example is emergency control. During emergencies, adsorption can control the pollution rapidly by taking in pollutants which are then further treated by advanced oxidation.

4. Restoration featuring environment-friendly titanium-based nanomaterials

4.1. Advantages of environment-friendly titanium-based nanomaterials

Building upon the earlier discussion, our objective is to identify an element that not just satisfies the requisites of photocatalytic oxidation but also mirrors the Fenton-like capabilities akin to Fe. A thorough analysis of transition metal elements within the periodic table reveals the vast potential of Ti element for the following reasons (Fig. 2) [71-73]:

(1) Similar electron structures: Ti and Fe belong to the fourth period elements, and their extranuclear electron structures are similar;
(2) Variable valence: Ti has variable valence ranging from 0 to +4 (0 for Ti foil, +2 for TiO, +3 for Ti_2O_3, +4 for TiO_2), and thus has a potential for Fenton-like catalysis;
(3) Rich reserves: China has the world's largest titanium ore reserves. They are estimated to be 200 million tons, which is 61 times as large as the copper reserves in the earth's crust;
(4) Environmental friendliness: Ti is recognized as a bio-friendly element, and commercial products containing Ti have already been widely seen in people's lives (such as sunscreen and titanium artificial bone).

For our future research endeavors, we will primarily focus on investigating conventional TiO_2 and innovative Ti_3C_2 MXene, typical Ti-based oxidizing nanomaterials, conducting comprehensive structural, physical, and chemical analyses. Our investigation aims to assess their effectiveness in eliminating pesticide-related emerging contaminants, identify prevailing challenges, and predict potential applications.

4.2. An overview of titanium-based photocatalytic oxidation

4.2.1. Titanium dioxide

Nano-titanium dioxide (n-TiO_2) stands out among various nano-photocatalysts for its widespread commercialization and popularity attributed to its cost-effectiveness, ease of operation, and remarkable performance. TiO_2-based nanocomposite material systems have found extensive application in the photocatalytic degradation of ECs from pesticides. The fundamental mechanism relies on the semiconductor's generation of oxidizing free radicals upon light exposure, facilitating the mineralization of pollutants [74]. Nevertheless, its extensive industrial utilization remains limited by challenges such as a wide band gap, high recombination rate, and low quantum yield of electron-hole pairs [75]. Consequently, numerous methods have been devised to address these inherent limitations.

Doping with metallic or nonmetallic elements, independently or combined, stands as an effective strategy to enhance its photoresponse. This method effectively reduces the band gap, facilitating catalysis even under low-energy visible or infrared light [76-78].

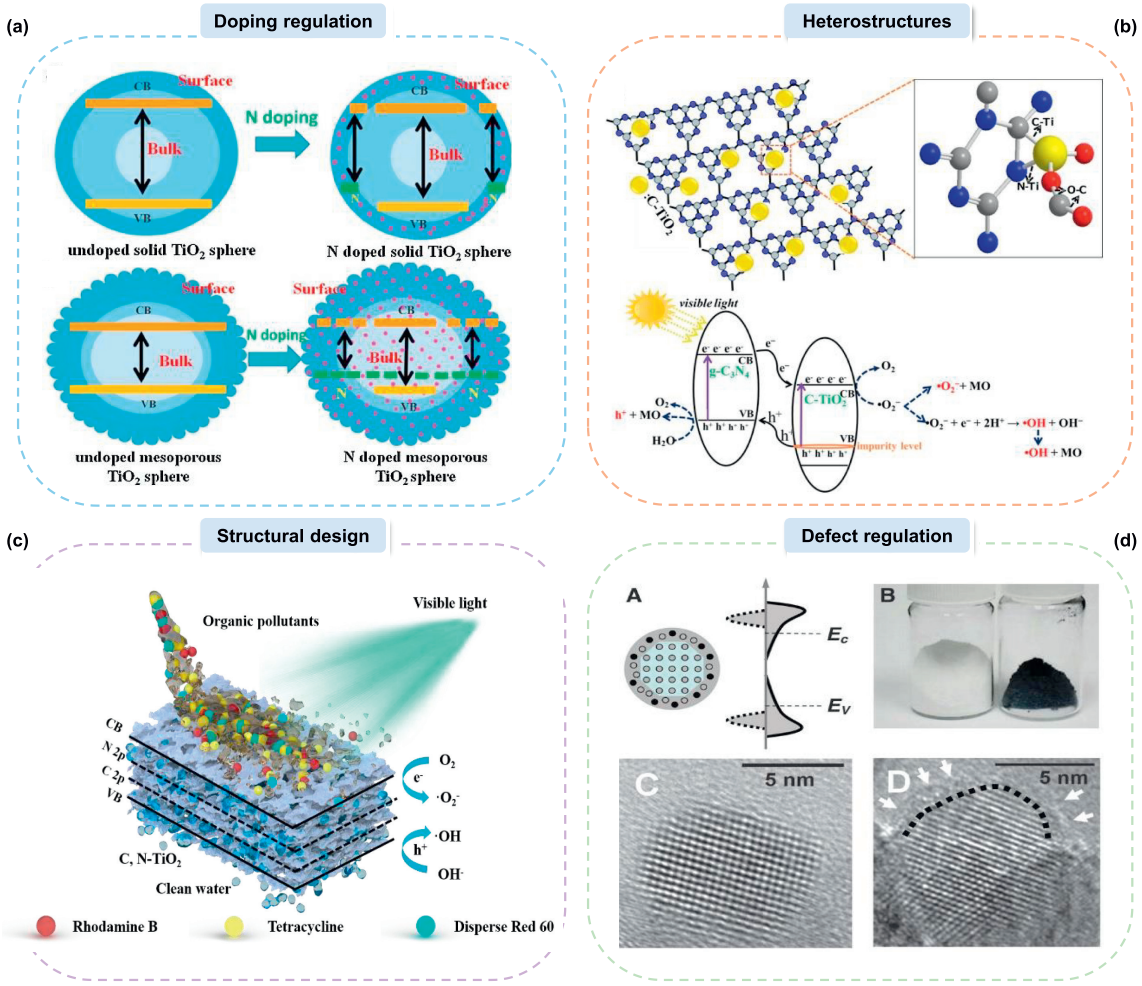

Fig. 3. Various strategies to improve the photocatalytic performances of Ti-based nanomaterials. (a) Doping regulation. Reprinted with permission [77]. Copyright 2015, Elsevier. (b) Heterostructures. Reprinted with permission [85]. Copyright 2017, Elsevier. (c) Structural design. Reprinted with permission [59]. Copyright 2021, Elsevier. (d) Defect regulation. Reprinted with permission [92]. Copyright 2011, American Association for the Advancement of Science.

Notably, nitrogen and tungsten doping introduce a new donor level beneath the material's conduction band, inducing a bathochromic shift towards visible light and significantly amplifying its photocatalytic prowess [79]. Photocatalytic activity measurements indicated a significant increase in atrazine degradation, achieving 90% within 4 h of visible light irradiation, compared to only 40% degradation using pristine TiO_2 [60]. Furthermore, carbon serves as a photosensitizer, heightening the material's absorption and responsiveness to visible light. Additionally, C-doping creates surface states that further narrow the band gap [80] and the addition of F element could also create more quantity of active {001} crystal facet. These effects are more favorable for the degradation of atrazine pesticides [81] (Fig. 3a).

Recent findings suggest that constructing heterostructures significantly enhances the separation rate of photo-generated electrons and holes, thereby bolstering the photocatalytic activity of semiconductors [82-84]. Various studies have successfully expedited the transfer rate of photo charges at interfaces through heterojunction design, yielding efficient visible-light active photocatalysts such as C-TiO_2/C_3N_4 [85] and heterojunction microspheres comprising g-C_3N_4/Ag/TiO_2 [86]. However, integrating additional components substantially inflates production costs. Hence, it would be more advantageous to develop heterostructures within the same material. It has been demonstrated that the separation rate of photogenerated electrons and holes can be optimized by adjusting the ratio of anatase to rutile in titanium dioxide. The highest atrazine degradation efficiency, 94.7%, is achieved in 180 min when the rutile content is 11.6% (Fig. 3b) [87].

Adapting and controlling the structure offers a promising solution. Crafting a three-dimensional lamellar porous configuration significantly amplifies the material's specific surface area, enhancing its ability to adsorb pollutants. This structural design serves a dual role: augmenting light reflectivity and refractive index within the pores, thereby intensifying light usage, while simultaneously shortening the path for photo-generated electrons and holes to reach the material's surface. This shortened distance reduces the likelihood of bulk phase recombination and facilitates the direct mineralization of pollutants on the surface. It often involves interactions with surface-bound molecules like O_2, fostering oxidation [88]. In addition, atrazine can strongly bind with Ti^{4+}, –O or –OH groups present on the TiO_2 surface (Fig. 3c) [89].

Beyond established methods like doping and structural adjustment, a contemporary approach called defect regulation has surfaced in recent years [90]. This technique involves precise adjustments to the atomic coordination number and electronic structure of the catalyst. Through this method, defect regulation fine-tunes the band gap of photocatalytic nanomaterials, enabling heightened utilization of both visible and infrared light spectrums. This process concurrently accelerates electron transfer rates, facilitating more efficient redox reactions [91]. Research indicates that defec-

tive titanium dioxide demonstrates superior performance in degrading pollutants (Fig. 3d) [92].

4.2.2. Transition metal carbide/nitride (MXene)

Since its inception in 2011, $Ti_3C_2T_x$, a two-dimensional transition metal carbide/nitride (MXene), has showcased remarkable developmental potential across its synthesis, characterization, and practical applications [93,94]. Currently, more than 70% of MXene research concentrates on $Ti_3C_2T_x$, establishing it as nearly synonymous with MXene materials. The general formula $M_{n+1}X_nT_x$ defines MXene, wherein M represents the transition metal, X signifies carbon or nitrogen, *n* varies from 1 to 4, and T_x designates the functional groups (*e.g.*, –OH, –F) present on the outermost layer of the transition metal [95].

In recent years, the utilization of MXene-based materials has surged in the domain of photocatalytic degradation of pollutants owing to their substantial specific surface area, high conductivity, hydrophilicity, and adaptable properties [96]. Investigations have revealed $Ti_3C_2T_x$'s proficient adsorption of the cationic dye methylene blue (MB) but its limited effectiveness with the anionic dye acid blue 80 (AB80). This disparity might be attributed to $Ti_3C_2T_x$'s inherent negative charge, facilitating preferential adsorption of pollutants bearing opposite charges. When subjected to UV irradiation, notable reductions of 81% in MB and 62% in AB80 concentrations were observed. However, prolonged irradiation inevitably oxidized $Ti_3C_2T_x$, converting it into TiO_2 and causing material degradation [97]. Consequently, the imperative focus remains on addressing the stability concerns of MXene-based materials.

The degradation efficiency of $Ti_3C_2T_x$ alone falls short of ideal standards. Thus, the creation of composite photocatalytic materials by pairing Ti_3C_2 MXene with Ag_3PO_4, leveraging the expansive surface area of Ti_3C_2, presents a viable approach. In the presence of light, the conductivity of Ti_3C_2 facilitates swift separation of photogenerated electrons and holes, curbing bulk phase recombination and augmenting the production of oxidizing free radicals. Overall, such composite photocatalytic materials exhibit promising degradation efficiency against tetracycline hydrochloride and chloramphenicol [98].

The research on MXene-based photocatalysts is still in its early stages. Until now, MXene has primarily served as a carrier and cocatalyst, especially in addressing simpler pollutants like dyes. While ongoing studies have highlighted the significant potential of MXene-based materials, particularly exemplified by Ti_3C_2, there is a critical need to further explore the inherent properties of TiO_2-based nanomaterials. Additionally, investigating techniques such as doping, structural adjustment/control, and defect engineering holds promise in providing controlled and efficient materials for real-world environmental pollutant degradation systems in the future.

4.2.3. Titanium-based metal organic frameworks (MOFs)

Metal-organic frameworks (MOFs) are porous crystalline materials composed of metals or metal-oxo clusters and organic linkers. They possess excellent characteristics such as intrinsic porosity, controllable size, ease of modification, and a large specific surface area [99,100]. These unique structural features make MOFs promising candidates for the adsorption and catalysis of pesticide contaminants. Among them, Ti-based MOFs stand out due to their low cost, non-toxicity, multifunctionality, biocompatibility, excellent redox activity (transitioning between Ti^{3+} and Ti^{4+}), and notable photocatalytic and photochemical properties [101-103].

Pesticide small molecule solvents, such as dichlorophenol (DCP) and trichlorophenol (TCP), were studied as representative contaminants. The removal efficiency of DCP and TCP was up to 93.28% and 92.19% by using mesoporous MIL-125-NH_2@Bi_2MoO_6 core-shell heterojunctions under visible light. This excellent photocatalytic performance can be attributed to the formation of core-shell heterojunctions and surface defects, which enhance charge separation and visible light absorption. Additionally, the mesoporous structure provides an ample number of surface active sites and facilitates mass transfer (Fig. 4a) [104]. Similarly, a Co-based MOF ($[Co_3(cis\text{-chhc})(H_2O)_6]_n$, Co-$H_6$chhc), as activator of PMS, was investigated to degrade ATZ. Under optimal conditions (pH = 5.5, PMS = 0.4 mmol/L, Co-H_6chhc = 300 mg/L, ATZ = 10 mg/L), the Co-H_6chhc/PMS system achieved 100% degradation of ATZ within 30 min. Co-H_6chhc demonstrated superior PMS activation and recyclability, maintaining a degradation efficiency of over 98% even after 5 cycles. Additionally, a fixed-bed reactor was constructed, which maintained an ATZ removal efficiency of over 90% after 72 h of continuous operation (Figs. 4b–d) [105].

4.3. An overview of titanium-based Fenton-like oxidation

Advanced oxidation processes (AOPs), employing traditional iron-based materials to catalyze hydrogen peroxide decomposition for in situ hydroxyl radical generation, have gained substantial traction in environmental restoration. However, iron precipitation remains a persistent challenge under strictly controlled acidic conditions in iron-based AOPs. Addressing this hurdle, our investigation focused on activating H_2O_2 using non-Fe-based Fenton catalysts in practical applications. These catalysts include elements exhibiting diverse redox states, such as aluminum [106], chromium [107], cerium [108], cobalt [109,110], manganese [111] and ruthenium [112]. Despite this progress, acknowledging the risk of heavy metal leakage and the necessity for a broad pH spectrum, further advancements are imperative to develop green and efficient Fenton-like catalysts [113].

In our prior investigations, we introduced a pioneering approach for *in-situ* fabricating Fenton-like nanocomposite catalysts, capitalizing on the inherent surface defects of MXene and enhancing the availability of transition metal sources (Fig. 5a) [114]. Using delaminated Ti_3C_2 MXene as a template, we synthesized a sequence of amorphous-carbon-supported high-density $TiO_{1.47}$ nanoclusters ($TiO_{1.47}$@C). Fine-tuning the preparation conditions (10 mol/L H_2O_2, 30 min) led to an exceptional sample yield (>97%) through adjustments in H_2O_2 concentration and reaction duration. Theoretical computations elucidated the pivotal role of surface Ti defects on Ti_3C_2 MXene as active sites, manifesting rich surface defects and Ti in diverse valence states (with an average valence state of +2.94). Analysis *via* X-ray absorption fine structure (XAFS) underscored that the *in-situ* oxidation of H_2O_2 during synthesis induced the rupture of Ti–C–Ti bonds and the formation of crucial Ti–O bonds, pivotal for the *in-situ* formation of nanoclusters. The $TiO_{1.47}$@C ([Ti] = 0.1 g/L) showed superior reactivity to activate H_2O_2 (5 mmol/L) to degrade atrazine (2.5 mg/L). More than 95% degradation efficiency can be achieved within 5 min. Unlike the conventional Fenton system, which typically results in substantial formation of Fe sludge post-reaction, $TiO_{1.47}$@C maintained a high degree of dispersion following degradation. Even after being left for 15 months, no precipitation was observed in the solution. The highly potentiated H_2O_2, altering the Ti valence, demonstrated remarkable efficacy in degrading various typical ECs (*e.g.*, tetracycline and *p*-nitrophenol. The chain reaction equations are detailed as follows:

$$Ti^{\delta+}{}_{Low} + H_2O_2 \rightarrow Ti^{\delta+}{}_{High} + OH^- + {}^{\bullet}OH \quad (17)$$

$$Ti^{\delta+}{}_{High} + H_2O_2 \rightarrow Ti^{\delta+}{}_{Low} + H^+ + HOO^{\bullet} \quad (18)$$

where, the $Ti^{\delta+}{}_{Low}$ denotes the low-valence state, the $Ti^{\delta+}{}_{High}$ denotes the low-valence state.

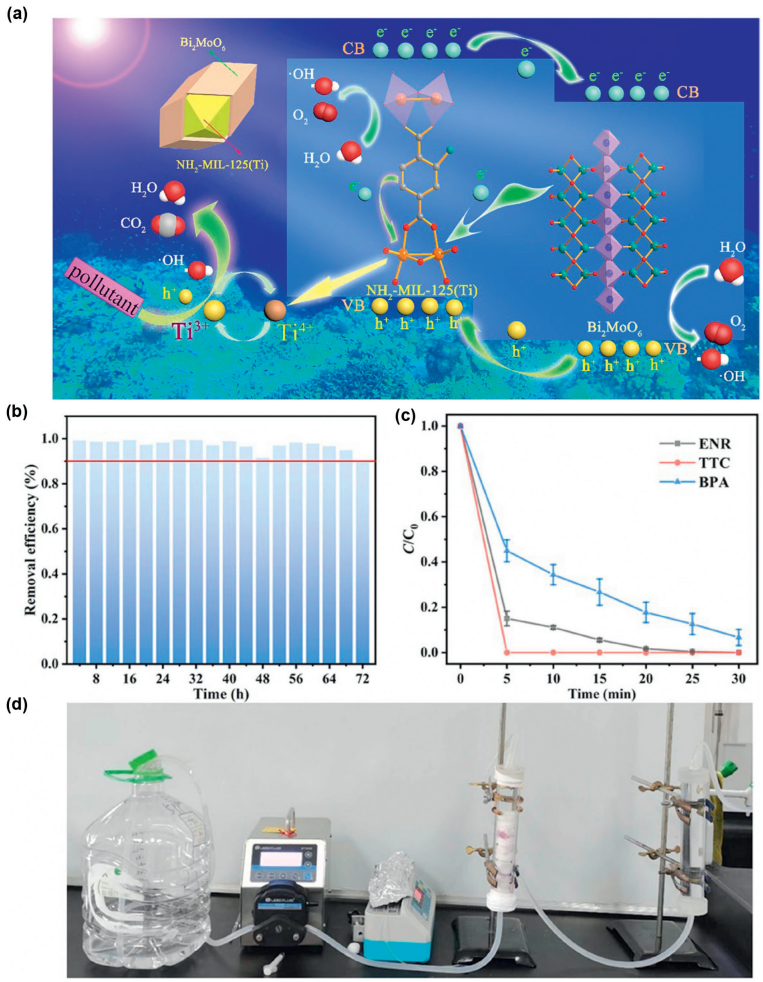

Fig. 4. (a) Illustration of the visible light-driven photocatalytic mechanism of NH_2-MIL-125(Ti)@Bi_2MoO_6 core-shell heterojunctions. Reproduced with permission [104]. Copyright 2019, Elsevier. (b) Long-term experiments on ATZ removal. (c) Degradation performance of different pollutants (*e.g.*, tetracycline (TC), enrofloxacin (ENR) and bisphenol A (BPA)) in Co-H_6chhc/PMS system. (d) Photograph of the fixed-bed device. Reaction conditions: ENR, TC, BPA = 10 mg/L, initial pH = 5.5, PMS = 0.4 mmol/L, Co-H_6chhc = 300 mg/L. Reprinted with permission [105]. Copyright 2023, Elsevier.

The method demonstrates universal applicability across diverse materials within the MXene family, including V_2C, Nb_2C, and related compounds. Our study significantly broadens the environmental potential of MXene-based materials, enabling the composite anchoring of nanoclusters onto carbon substrates. This process facilitates the *in-situ* synthesis of highly active nanoclusters while effectively mitigating potential environmental risks associated with material leakage during treatment. Additionally, through concrete examples, we have outlined "Safer-by-design" strategies for the production of two-dimensional nanomaterials, presenting an innovative approach for the efficient treatment of ECs, such as endocrine disruptors and antibiotics. In addition to H_2O_2 as an oxidizing agent, peroxymonosulfate [115] and peroxyacetic acid (PAA) [116,117] are discussed in detail. PMS facilitated the degradation of ATZ in the durable hollow core-shell TiO_2@$LaFeO_3$/PMS system by acting both as an electron trapper and a radical precursor. This dual function enabled efficient capture of photogenerated charges by PMS, initiating the production of reactive oxygen species. Additionally, photogenerated electrons from the photocatalyst interacted with PMS, breaking the peroxide bond to form $SO_4^{\bullet-}$. However, $SO_4^{\bullet-}$ was not the primary oxidant in this system. Instead, PMS primarily promoted the continuous extraction of photogenerated electrons through three-dimensional channels. This process inhibited electron-hole recombination and minimized energy loss during photocatalysis, thereby extending the lifetime of photogenerated charge carriers. As a result, more holes were available for the generation of ·OH radicals, enhancing the removal of ATZ (Fig. 5b) [118]. Similar catalytic mechanisms were similarly discussed in photo-fenton catalysis (Fig. 5c) [65]. More interestingly, a nonradical oxidation process induced by Ti-peroxo complex was further discussed, which showed a higher specificity toward the degradation of tetracycline antibiotics (Fig. 5d) [119]. Nonradical oxidative pathways may serve as a favorable complement to free radical catalytic pathways.

5. Outlook

Significant strides have been achieved in constructing, enhancing catalytic efficiency, and conducting mechanistic studies of advanced oxidation systems using eco-friendly nanomaterials. However, pivotal challenges persist, warranting further examination in future research:

(1) The experimental pollutant concentrations often exceed mg/L, surpassing typical environmental levels. Future studies ought to target trace pollutants inherent to natural environments, while addressing the impact of common ions and humic acids on reaction systems;
(2) Present experiments commonly focus on degrading individual pollutants in laboratory water settings. Future investigations

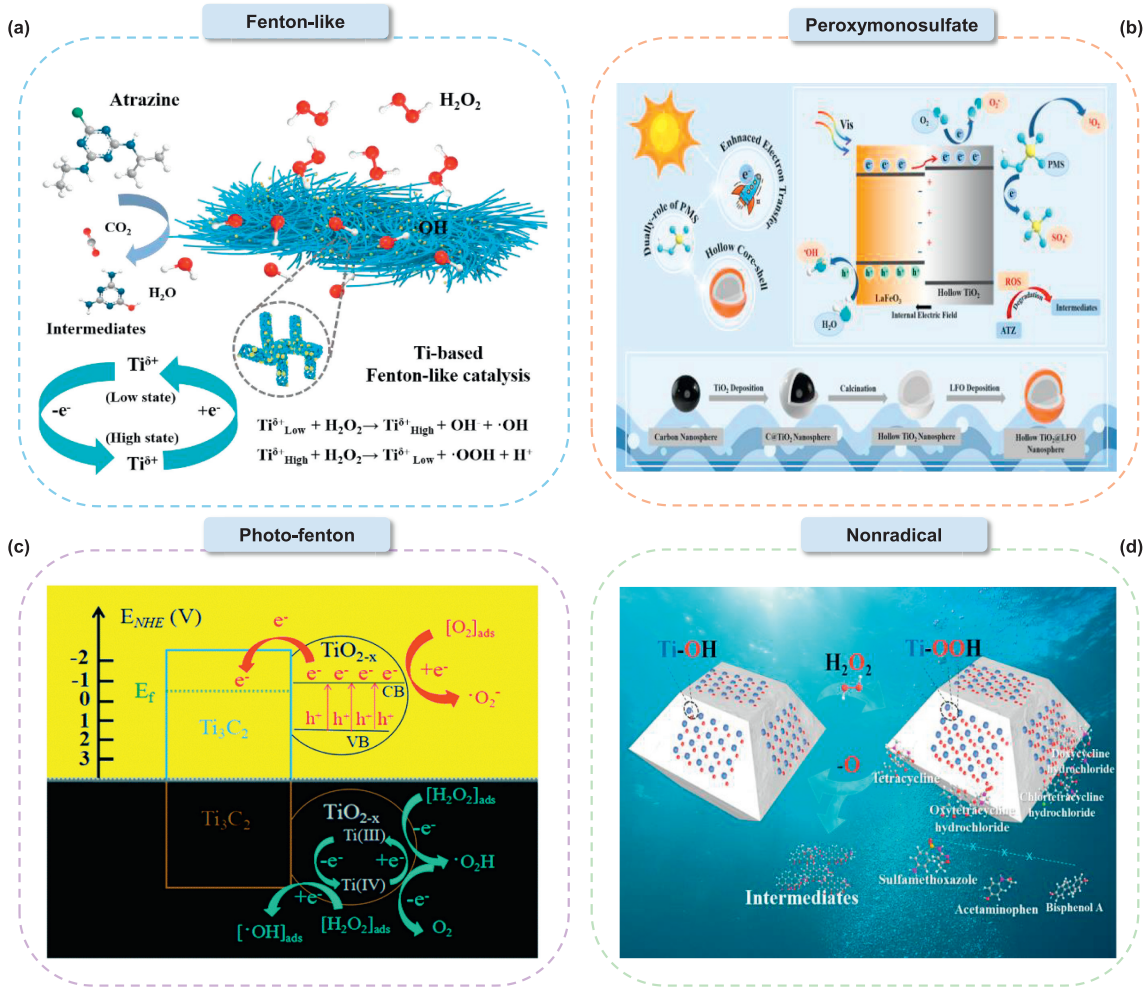

Fig. 5. Ti-based Fenton-like processes. The H_2O_2-induced Fenton-like reactions (a) and peroxymonosulfate process (b). Reproduced with permission [114]. Copyright 2023, National Academy of Science. Reprinted with permission [118]. Copyright 2022, Elsevier. (c) Photo-Fenton catalysis. Reproduced with permission [65]. Copyright 2018, Royal Society of Chemistry. (d) Nonradical oxidation process. Reprinted with permission [119]. Copyright 2023, Elsevier.

should delve into the simultaneous degradation of multiple pollutants within a composite system. Furthermore, evaluating water samples from natural environments can effectively assess the practical feasibility of implementing this reaction system in real-world scenarios;

(3) The design of materials should be closely focused on tackling the actual environmental issues, which means that the EFMs should be designed according to actual needs with special attention paid to the stability of materials;

(4) In future, more in-depth data processing and analysis techniques are required for *in-situ* observation and characterization of catalyzed reactions, preferably combined with *in-situ* XAFS, infrared, Raman, and other techniques;

(5) Efforts towards integrating diverse computational models demand attention. Recent observations highlight shifts in the bonding energy of pollutants upon surface absorption onto materials. Relying solely on the Gaussian model for simulating pollutant bond breakage lacks precision due to these alterations. An integrated approach that melds Gaussian and VASP models is crucial. Additionally, employing theoretical calculations effectively can significantly enhance their alignment with actual experimental data;

(6) Heightened attention should be devoted to the potential environmental risks presented by materials, pollutants, and reaction intermediates. The design and utilization of materials should inherently embody the principles of "Safer-by-design" and "Sustainable-by-design". The "Safer-by-design" strategy strives to develop materials that are less toxic and more environmentally friendly during the design phase of innovation. "Sustainable-by-design" extends this approach, integrating sustainability considerations into materials/products and their associated processes throughout the entire life cycle;

(7) In future research, it is imperative to assess the utility of environmentally functional materials from a holistic standpoint, encompassing comprehensive analyses such as cradle-to-cradle life cycle assessment, economic evaluation, carbon footprint analysis, and other strategic means of effective utilization.

Declaration of competing interest

The authors declare that they have no known competing financial interests or personal relationships that could have appeared to influence the work reported in this paper.

CRediT authorship contribution statement

Chu Wu: Writing – original draft, Investigation, Formal analysis. **Zhichao Dong:** Writing – original draft, Investigation, Formal analysis. **Jinfang Hou:** Investigation, Formal analysis. **Jian Peng:** Investigation, Formal analysis, Data curation. **Shuangyu Wu:** Investi-

gation, Formal analysis, Data curation. **Xiaofang Wang:** Investigation, Formal analysis. **Xiangwei Kong:** Investigation, Formal analysis. **Yue Jiang:** Writing – review & editing, Writing – original draft, Funding acquisition.

Acknowledgments

This work was supported by the Research Platform Open Fund Project of Zhejiang Industry and Trade Vocation College (No. Kf202203), the Scientific Research Project of CCCC First Harbor Engineering Company Ltd. (No. 2022-7-2), the National Natural Science Foundation of China (No. 22406142), the Fellowship of China National Postdoctoral Program for Innovative Talents (No. BX20230262), the Fellowship of China Postdoctoral Science Foundation (No. 2023M732636) and the Shanghai Post-doctoral Excellence Program (No. 2023755). The authors are especially grateful to the Dr. Jiazhen Cao for her help in revising the graphics.

Supplementary materials

Supplementary material associated with this article can be found, in the online version, at doi:10.1016/j.cclet.2024.110438.

References

[1] S. Khan, M. Naushad, M. Govarthanan, et al., Environ. Res. 207 (2022) 112609.
[2] H. Ramirez-Malule, D.H. Quinones-Murillo, D. Manotas-Duque, Emerg. Contam. 6 (2020) 179–193.
[3] B. Wang, G. Yu, Front. Environ Sci. Eng. 16 (2022) 81.
[4] J.A. Downing, S. Polasky, S.M. Olmstead, et al., Nat. Commun. 12 (2021) 2709.
[5] J. Guo, K. Tu, L. Chou, et al., Water Res. 243 (2023) 120318.
[6] B. Yilmaz, H. Terekeci, S. Sandal, et al., Rev. Endocr. Metab. Disord. 21 (2020) 127–147.
[7] Y. Peng, W. Fang, M. Krauss, et al., Environ. Pollut. 241 (2018) 484–493.
[8] W.A. Battaglin, K.L. Smalling, C. Anderson, et al., Sci. Total Environ. 566 (2016) 320–332.
[9] H.K.L. Johansson, T. Svingen, P.A. Fowler, et al., Nat. Rev. Endocrinol. 13 (2017) 400–414.
[10] N.E. Skakkebaek, Horm. Res. Paediatr. 86 (2016) 240–246.
[11] A. Ghassabian, L. Trasande, Front. Endocrinol. 9 (2018) 204.
[12] P. Alonso-Magdalena, E. Vieira, S. Soriano, et al., Environ. Health Perspect. 118 (2010) 1243–1250.
[13] M. Giulivo, M.L. de Alda, E. Capri, et al., Environ. Res. 151 (2016) 251–264.
[14] M.A. La Merrill, L.N. Vandenberg, M.T. Smith, et al., Nat. Rev. Endocrinol. 16 (2020) 45–57.
[15] K. Fenner, S. Canonica, L.P. Wackett, et al., Science 341 (2013) 752–758.
[16] P.J.J. Alvarez, C.K. Chan, M. Elimelech, et al., Nat. Nanotechnol. 13 (2018) 634–641.
[17] S.F. Hansen, R. Arvidsson, M.B. Nielsen, et al., Nat. Nanotechnol. 17 (2022) 682–685.
[18] A.A. Keller, A. Ehrens, Y. Zheng, et al., Nat. Nanotechnol. 18 (2023) 834–837.
[19] X. Zhao, F. Ma, C. Feng, et al., J. Biotechnol. 248 (2017) 43–47.
[20] T. El Sebai, M. Devers-Lamrani, F. Changey, et al., Int. Biodeterior. Biodegrad. 65 (2011) 1249–1255.
[21] J. Wang, L. Zhu, Q. Wang, et al., PLoS One 9 (2014) e107270.
[22] A.F. Tonelli Fernandes, V.S. Braz, A. Bauermeister, et al., Int. Biodeterior. Biodegrad. 130 (2018) 17–22.
[23] X. Zhao, L. Wang, F. Ma, et al., J. Environ. Sci. 54 (2017) 152–159.
[24] L. Ma, S. Chen, J. Yuan, et al., Int. Biodeterior. Biodegrad. 116 (2017) 133–140.
[25] P. Bhardwaj, A. Sharma, S. Sagarkar, et al., Biochem. Eng. J. 102 (2015) 125–134.
[26] J. Wang, L. Zhu, A. Liu, et al., Environ. Geochem. Health 33 (2011) 259–266.
[27] Y. Dai, K. Zhang, J. Li, et al., Sep. Purif. Technol. 186 (2017) 255–263.
[28] J. Cao, Z. Xu, Y. Chen, et al., Angew. Chem. Int. Ed. 135 (2023) e202302202.
[29] J.O. Ighalo, A.G. Adeniyi, A.A. Adelodun, J. Ind. Eng. Chem. 93 (2021) 117–137.
[30] C. Peiris, S.R. Gunatilake, T.E. Mlsna, et al., Bioresour. Technol. 246 (2017) 150–159.
[31] J.M. Park, S.H. Jhung, J. Hazard. Mater. 396 (2020) 122624.
[32] F. Suo, X. You, Y. Ma, et al., Chemosphere 235 (2019) 918–925.
[33] W. Zheng, M. Guo, T. Chow, et al., J. Hazard. Mater. 181 (2010) 121–126.
[34] P.N. Chandra, K. Usha, in: International Conference on Management and Recycling of Metallurgical Wastes (MetWaste-2020), Varanasi, India, 2020.
[35] A.L. Ahmad, L.S. Tan, S.R.A. Shukor, J. Hazard. Mater. 151 (2008) 71–77.
[36] P.E. Stackelberg, J. Gibs, E.T. Furlong, et al., Sci. Total Environ. 377 (2007) 255–272.
[37] N.M. Vieno, H. Harkki, T. Tuhkanen, et al., Environ. Sci. Technol. 41 (2007) 5077–5084.
[38] V.K. Sharma, Chemosphere 73 (2008) 1379–1386.
[39] M. Deborde, U. von Gunten, Water Res. 42 (2008) 13–51.
[40] J.L. Acero, F.Javier Benitez, F.J. Real, et al., Water Res. 44 (2010) 4158–4170.
[41] B. Ye, Z. Liu, X. Zhu, et al., Chem. Eng. J. 415 (2021) 128841.
[42] X. Kong, L. Wang, Z. Wu, et al., Water Res. 177 (2020) 115784.
[43] H. Stockinger, E. Heinzle, O.M. Kut, Environ. Sci. Technol. 29 (1995) 2016–2022.
[44] R. Andreozzi, V. Caprio, A. Insola, et al., Catal. Today 53 (1999) 51–59.
[45] X. Yuan, R. Xie, Q. Zhang, et al., Sep. Purif. Technol. 211 (2019) 823–831.
[46] D. Wang, H. Xu, J. Ma, et al., Chem. Eng. J. 354 (2018) 113–125.
[47] A.L. Boreen, W.A. Arnold, K. McNeill, Environ. Sci. Technol. 38 (2004) 3933–3940.
[48] I. Arslan-Alaton, S. Dogruel, J. Hazard. Mater. 112 (2004) 105–113.
[49] D.L. Giokas, A.G. Vlessidis, Talanta 71 (2007) 288–295.
[50] Y. Yang, C. Shan, B. Pan, Water Res. 255 (2024) 121484.
[51] X.A.M. Mutke, P. Swiderski, F. Drees, et al., Water Res. 255 (2024) 12146.
[52] X. Kong, J. Jiang, J. Ma, et al., Water Res. 90 (2016) 15–23.
[53] M. Panizza, G. Cerisola, Chem. Rev. 109 (2009) 6541–6569.
[54] B. Balci, N. Oturan, R. Cherrier, et al., Water Res. 43 (2009) 1924–1934.
[55] X. Chen, X. Hu, L. An, et al., Electrocatalysis 5 (2014) 68–74.
[56] D.A. Armstrong, R.E. Huie, W.H. Koppenol, et al., Pure Appl. Chem. 87 (2015) 1139–1150.
[57] L. Chen, X. Hu, Y. Yang, et al., Chem. Eng. J. 351 (2018) 523–531.
[58] S. Wu, H. He, X. Li, et al., Chem. Eng. J. 341 (2018) 126–136.
[59] Y. Jiang, Y. Qin, T. Yu, et al., Chin. Chem. Lett. 32 (2021) 1823–1826.
[60] C. Belver, C. Han, J.J. Rodriguez, et al., Catal. Today 280 (2017) 21–28.
[61] H. Sudrajat, P. Sujaridworakun, J. Mol. Liq. 242 (2017) 433–440.
[62] J.M. Britto, M.d.C. Rangel, Quim. Nova 31 (2008) 114–122.
[63] F. Haber, J. Weiss, Sci. Nat. 20 (1932) 948–950.
[64] W.G. Barb, J.H. Baxendale, P. George, et al., Nature 163 (1949) 692–694.
[65] X. Cheng, L. Zu, Y. Jiang, et al., Chem. Comm. 54 (2018) 11622–11625.
[66] Z. Chen, F. An, Y. Zhang, et al., Proc. Natl. Acad. Sci. U. S. A. 120 (2023) e2305933120.
[67] C. Wang, Z. Guo, R. Hong, et al., Chemosphere 197 (2018) 576–584.
[68] C. Wang, R. Sun, R. Huang, H. Wang, Sep. Purif. Technol. 270 (2021) 118773.
[69] Z. Xie, C. Wang, L. Yin, J. Catal. 353 (2017) 11–18.
[70] S. Lin, T. Yu, Z. Yu, et al., Adv. Mater. 30 (2018) 1705691.
[71] W. Fang, M. Xing, J. Zhang, J. Photochem. Photobio. C 32 (2017) 21–39.
[72] K.T. Kim, M.Y. Eo, N. Truc Thi Hoang, et al., Int. J. Dent. 5 (2019) 10.
[73] K. Liu, M. Cao, A. Fujishima, et al., Chem. Rev. 114 (2014) 10044–10094.
[74] F. Saadati, N. Keramati, M.M. Ghazi, Crit. Rev. Environ. Sci. Technol. 46 (2016) 757–782.
[75] J. Schneider, M. Matsuoka, M. Takeuchi, et al., Chem. Rev. 114 (2014) 9919–9986.
[76] Q. Zhang, D.Q. Lima, I. Lee, et al., Angew. Chem. Int. Ed. 50 (2011) 7088–7092.
[77] X. Wang, T.T. Lim, Appl. Catal. A 399 (2011) 233–241.
[78] S. Modi, V.K. Yadav, A. Amari, et al., Water 15 (2023) 2275.
[79] R. Asahi, T. Morikawa, H. Irie, et al., Chem. Rev. 114 (2014) 9824–9852.
[80] M. Nolan, A. Iwaszuk, A.K. Lucid, et al., Adv. Mater. 28 (2016) 5425–5446.
[81] Y. Zhang, C. Han, M.N. Nadagouda, et al., Appl. Catal. B 168 (2015) 550–558.
[82] T. Wang, C. Zhao, L. Meng, et al., Appl. Catal. B 334 (2023) 122832.
[83] L. Meng, C. Zhao, T. Wang, et al., Sep. Purif. Technol. 313 (2023) 123511.
[84] X. Wei, S. Naraginti, P. Chen, et al., Water 15 (2023) 3702.
[85] Z. Lu, L. Zeng, W. Song, et al., Appl. Catal. B 202 (2017) 489–499.
[86] Y. Chen, W. Huang, D. He, et al., ACS Appl. Mater. Interfaces 6 (2014) 14405–14414.
[87] W.K. Wang, J.J. Chen, M. Gao, et al., Appl. Catal. B 195 (2016) 69–76.
[88] J. Fei, J. Li, Adv. Mater. 27 (2015) 314–319.
[89] S. Parra, S.E. Stanca, I. Guasaquillo, et al., Appl. Catal. B 51 (2004) 107–116.
[90] G. Ou, Y. Xu, B. Wen, et al., Nat. Commun. 9 (2018) 1302.
[91] S.G. Ullattil, S.B. Narendranath, S.C. Pillai, et al., Chem. Eng. J. 343 (2018) 708–736.
[92] X. Chen, L. Liu, P.Y. Yu, et al., Science 331 (2011) 746–750.
[93] M. Naguib, M. Kurtoglu, V. Presser, et al., Adv. Mater. 23 (2011) 4248–4253.
[94] M.R. Lukatskaya, S. Kota, Z. Lin, et al., Nat. Energy 2 (2017) 17105.
[95] M. Naguib, M.W. Barsoum, Y. Gogotsi, Adv. Mater. 33 (2021) 2103393.
[96] J. Peng, X. Chen, W.J. Ong, et al., Chem 5 (2019) 18–50.
[97] O. Mashtalir, K.M. Cook, V.N. Mochalin, et al., J. Mater. Chem. A 2 (2014) 14334–14338.
[98] T. Cai, L. Wang, Y. Liu, et al., Appl. Catal. B 239 (2018) 545–554.
[99] A. Du, H. Fu, P. Wang, et al., Chemosphere 322 (2023) 138221.
[100] Y.C. Zhou, P. Wang, H. Fu, et al., Chin. Chem. Lett. 31 (2020) 2645–2650.
[101] N.S.A. Mubarak, K.Y. Foo, R. Schneider, et al., J. Environ. Chem. Eng. 10 (2022) 106883.
[102] Y.X. Li, X. Wang, C.C. Wang, et al., J. Hazard. Mater. 399 (2020) 123085.
[103] C. Zhao, Z. Wang, X. Chen, et al., Chin. J. Catal. 41 (2020) 1186–1197.
[104] S. Zhang, M. Du, J. Kuang, et al., J. Colloid Interface Sci. 554 (2019) 324–334.
[105] Y. Li, F. Wang, X. Ren, et al., J. Environ. Chem. Eng. 11 (2023) 109116.
[106] H.L. Lien, W.X. Zhang, J. Environ. Eng. 128 (2002) 791–798.
[107] A.D. Bokare, W. Choi, Environ. Sci. Technol. 44 (2010) 7232–7237.
[108] E.G. Heckert, S. Seal, W.T. Self, Environ. Sci. Technol. 42 (2008) 5014–5019.
[109] Y. Pan, J. Cao, M. Xing, Y. Zhang, ACS EST Eng. 4 (2023) 19–46.
[110] J. Ji, Q. Yan, P. Yin, et al., Angew. Chem. Int. Ed. 60 (2021) 2903–2908.
[111] R.J. Watts, J. Sarasa, F.J. Loge, et al., J. Environ. Eng. 131 (2005) 158–164.

[112] Z. Hu, C.F. Leung, Y.K. Tsang, New J. Chem. 35 (2011) 149–155.
[113] A.D. Bokare, W. Choi, J. Hazard. Mater. 275 (2014) 121–135.
[114] Y. Jiang, D. Baimanov, S. Jin, et al., Proc. Natl. Acad. Sci. U. S. A. 120 (2023) e2210211120.
[115] F. Wang, S.S. Liu, Z. Feng, et al., J. Hazard. Mater. 440 (2022) 129723.
[116] T. Liu, S. Xiao, N. Li, et al., Nat. Commun. 14 (2023) 2881.
[117] F. Chen, Y.J. Sun, X.T. Huang, et al., Proc. Natl. Acad. Sci. U. S. A. 121 (2024) e2314396121.
[118] K. Wei, A. Armutlulu, Y. Wang, et al., Appl. Catal. B 303 (2022) 120889.
[119] J. Peng, Y. Jiang, S. Wu, et al., Chin. Chem. Lett. 35 (2024) 108903.